

# Numerical Modelling of a Loop-Type Heat Pipe Suitable for the Reactor Cavity Cooling System of the Pebble Bed Modular Reactor

R. T. Dobson and I. Sittmann

Department of Mechanical Engineering, University of Stellenbosch

Private Bag X1, MATIELAND 7602, South Africa

Tel: +27 21 808 4286, Fax: +27 20 808 4958, E-mail: [rtd@sun.ac.za](mailto:rtd@sun.ac.za)

## Abstract

The feasibility of a closed loop thermosyphon for the Reactor Cavity Cooling System (RCCS) of the Pebble Bed Modular Reactor has been the subject of many research projects. One of the difficulties identified by previous studies is the precise applicability of appropriate heat transfer coefficient correlations available in literature. This article presents the numerical modelling of the current design of the RCCS, incorporating single phase inside-pipe heat transfer coefficient correlations developed by the author. A one-third-height-scale model of the RCCS was designed and manufactured on which twelve experiments, lasting at least 5 hours each, were performed. The experimental results obtained, were used to verify the theoretical model.

*Key Words: Closed loop thermosyphons, heat transfer coefficients, two-phase flow modelling, reactor cavity cooling system, pebble bed modular reactor*

## 1. INTRODUCTION

The Pebble Bed Modular Reactor (PBMR) concept evolved from a German high temperature, helium-cooled reactor design with ceramic spherical fuel elements known as INTERATOM HTR-MODUL. The main advantage of this design is that the reactor can be continuously refuelled during operation. The most noted safety feature of this design is that the silicon carbide coating of the fuel particle within the pebbles provides the first level of containment, as it keeps the fission products within itself. Containment integrity is contained under all operating conditions. These design features facilitate the removal of parasitic heat through the Reactor Cavity Cooling System (RCCS).

The RCCS's primary function is to maintain the cavity temperature within a required range. This provides protection to the concrete structures surrounding the reactor and also, during loss of coolant

accident operating conditions, transports parasitic heat from the reactor to the environment [1].

The current RCCS for the PBMR, as proposed by Dobson (2006), is given in Figure 1. The RCCS, in this concept, is represented by a number of axially symmetrical elements: the reactor core, reactor pressure vessel, air in the cavity between the reactor vessel and the concrete structure, the concrete structure, a heat sink situated outside the concrete structure, and a number of closed loop thermosyphons with the one vertical leg in the hot air cavity and the other leg in the heat sink. These loops are spaced around the periphery of the reactor cavity at a pitch angle  $\theta$ . Vertical fins are attached to the length of the pipe in the cavity in order to shield the concrete structure from radiation and convection (from the reactor vessel through the gap between the pipes) and to conduct the heat to the pipes [2].

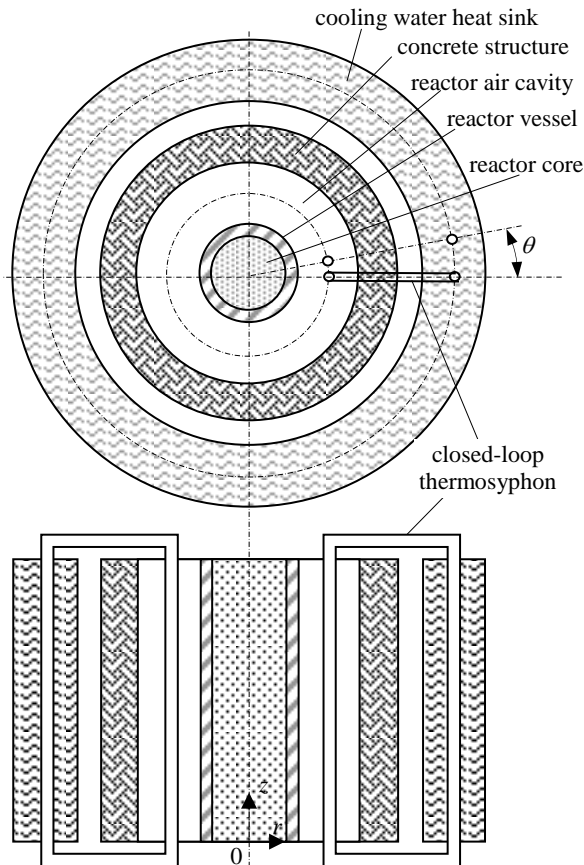


Figure 1: RCCS concept (Dobson, 2006)

## 2. EXPERIMENTAL MODEL

A one-third-height-scale model of the RCCS was designed and manufactured. Figure 2 shows the experimental setup, the orifice plate, heat exchangers, heating elements and pressure transducers. Note that the loop is rectangular in one plane, the apparent distortion is due to the wide angle camera lens. Figure 3 shows a schematic representation of the thermosyphon loop constructed for the experimental setup.

Each experiment followed the same heat input procedure. During start-up, each heating element was set to 30% of maximum power input. The working fluid temperature was monitored and the power input maintained until thermal equilibrium was reached. At that stage, the power input was increased to 50% and the process repeated. The same was done for 70%, as

well as full power conditions. The power supply was then switched off and the system was allowed to cool for one hour with the cooling water running and then the water supply was switched off. The system was then left to return to initial conditions and the next experiment was only started once the loop was in thermal equilibrium with its surroundings.

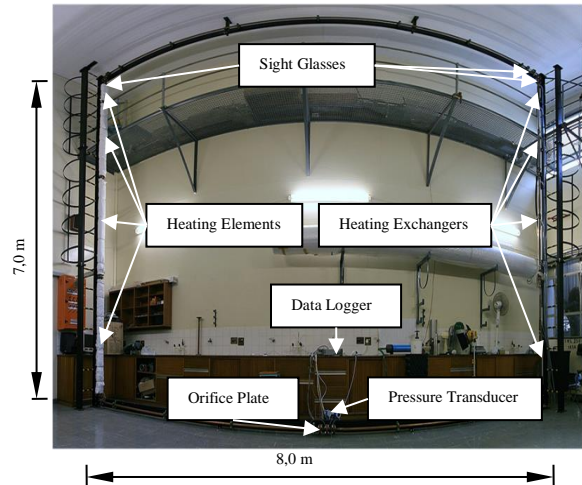


Figure 2: Experimental setup with element covers removed (taken with a wide angle lens)

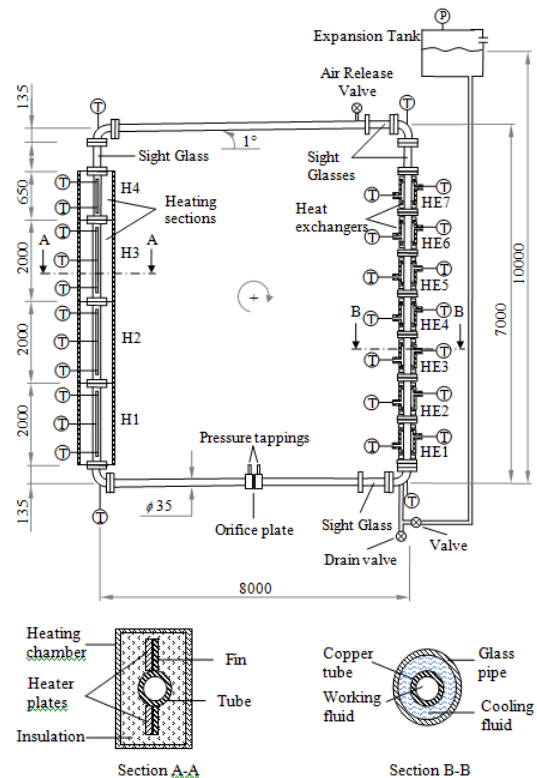


Figure 3: Thermosyphon loop

### 3. THEORETICAL MODEL

The mathematical model was developed subject to the following assumptions: the thermodynamic process is quasi-static; compressibility effects due to heating or cooling of the liquid and vapour phases are negligible; and that the flow is one-dimensional. The RCCS was modelled as a one-dimensional system using the homogenous flow model. Figure 4 shows the discretised system: the thermosyphon, evaporator section, condenser section, and expansion tank divided into control volumes.

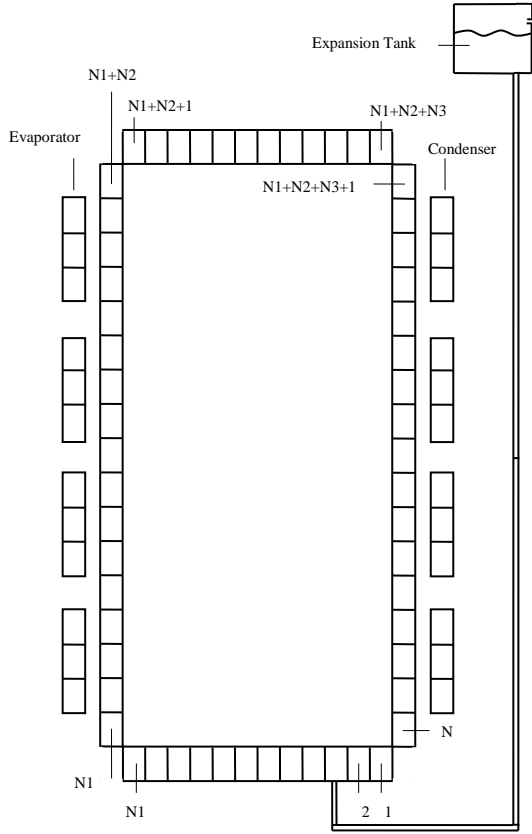


Figure 4: The one dimensional discretised theoretical model of the RCCS

Assuming that the mixture mass is constant across the control volume and with the quasi-static assumption, the mixture energy conservation equation [3] can be written as a difference equation for the working fluid:

$$T_m^{t+\Delta t} = T_m^t + \frac{\Delta t \dot{S}}{2m_m c_{v,m}} - \frac{\Delta t \dot{m}_m}{2m_m c_{v,m}} (h_{m,out} - h_{m,in})$$

$$-\Delta t \frac{\Delta C_{v,m}}{\Delta t} \left( \frac{T_m}{C_{v,m}} \right) - \Delta t \frac{\Delta m_m}{\Delta t} \left( \frac{T_m}{m_m} \right) \quad (1)$$

In equation (1),  $\dot{S}$  represents the heat transferred across the control volume boundaries. The new temperature allows the calculation of the internal energy and quality at each time-step [4]:

$$\begin{aligned} \text{If } T_m^{t+\Delta t} < T_{sat} \text{ then} \\ u_m^{t+\Delta t} = C_{v,m} T_m^{t+\Delta t} \quad \text{and} \\ x^{t+\Delta t} = 0 \end{aligned} \quad (2)$$

$$\begin{aligned} \text{If } T_m^{t+\Delta t} > T_{sat} \text{ then} \\ T_m^{t+\Delta t} = T_{sat}, \quad u_m^{t+\Delta t} = C_{v,m} T_m^{t+\Delta t} \quad \text{and} \\ x^{t+\Delta t} = \frac{u_m^{t+\Delta t} - u_f^{t+\Delta t}}{u_{fg}^{t+\Delta t}} \end{aligned} \quad (3)$$

Assuming a constant mass flow rate across the control volume and a constant cross-sectional area, the mixture momentum conservation equation [3] for the working fluid can be written as a difference equation:

$$\begin{aligned} v_m^{t+\Delta t} = v_m^t \\ + \Delta t \left( -\sum \left( \frac{f}{4} + k \right) \frac{\dot{m}^2 A_z}{2\bar{\rho}^2 A_x^3 L} \sum g \sin \theta \right) \\ - \frac{\bar{\rho}^t - \bar{\rho}^{t-\Delta t}}{\Delta t} \sum \frac{\dot{m}}{\bar{\rho}^2 A_x L} \end{aligned} \quad (4)$$

The new velocity allows for the calculation of the mass flow rate at each time-step.

In order to determine how much mass is transferred to or from the expansion tank, it is necessary to apply the mass conservation equation [13] as a difference equation:

$$m_m^{t+\Delta t} = m_m^t + \Delta t (\dot{m}_{t,i-1} - \dot{m}_{t,i}) \quad (5)$$

The new mixture mass, in conjunction with the new quality, allows for the calculation of the new phase masses by using the following identities [15]:

$$m_v = x m_m \quad (6)$$

$$m_l = (1 - x) m_m \quad (7)$$

The new phase volumes for a control volume can be used to calculate the new mixture volume:

$$V_k = \frac{m_k}{\rho_k} \quad (8)$$

$$V_m = V_l + V_v \quad (9)$$

The control volume retains a constant volume. The change in mixture volume is compensated for by the expansion tank.

### 3.1 Friction Factor

Crowe, Elger & Roberson (2001) give correlations for the laminar and turbulent friction factor for flow in conduits [6]. The resistance coefficient for laminar, fully developed flow (smooth surface) is given by:

$$f = \frac{64}{Re_D} \quad Re_D > 2000 \quad (10)$$

For turbulent flow, analytical and empirical results using smooth pipes give an approximate correlation for the friction factor [16]:

$$\frac{1}{\sqrt{f}} = 2 \log(Re_D \sqrt{f}) - 0.8 \quad Re_D > 3000 \quad (11)$$

An explicit equation for the friction factor was developed that differs less than 3% from the Moody diagram predictions for  $4 \times 10^3 < Re_D < 10^8$  and  $10^{-5} < \frac{k_s}{D} < 2 \times 10^{-2}$ .

$$f = \frac{0.25}{\left[ \log_{10} \left( \frac{k_s}{3.7D} + \frac{5.74}{Re_D^{0.9}} \right) \right]^2} \quad (12)$$

### 3.2 Heat Transfer Correlations

The researcher developed single phase inside-pipe heat transfer coefficients for both the evaporator and condenser sections specific to the given experimental conditions.

For single phase flow in the evaporator section, a power law correlation, generated using 5783 experimental data points, is used to calculate the bulk Nusselt number:

$$Nu_b = 1.3 \times 10^8 Re_q^{1.954} Pr^{0.340} Gr^{-0.835} \quad (13)$$

The average single phase Nusselt number is calculated from adjusting equation 13 using the viscosity ratio [7]:

$$\frac{Nu}{Nu_b} = \left( \frac{\mu_s}{\mu_b} \right)^{-0.11} \quad (14)$$

The single phase inside-pipe evaporator heat transfer coefficient is then calculated using [7]:

$$h_{e,i} = \frac{Nu k_l}{D} \quad (15)$$

For two-phase boiling in the evaporator section, Chen's correlation [5] will be used:

$$h = h_{NB} + h_{FC} = Sh_{FZ} + Fh_l \quad (16)$$

In equation 16,  $h_l$  is the researcher's generated single phase inside-pipe evaporator heat transfer coefficient.

For single phase flow in the condenser section, a power law correlation, generated using 9215 experimental data points, will be used to calculate the bulk Nusselt number:

$$Nu_b = 0.579 Re_q^{0.538} Pr^{1.094} \quad (17)$$

Finally, for two-phase condensation in the condenser section, the correlation proposed by Shah [9] is used:

$$\frac{h}{h_{lo}} = (1-x)^{0.8} + \frac{3.8 \cdot x^{0.76} \cdot (1-x)^{0.04}}{Pr^{0.38}} \quad (18)$$

In equation 18,  $h_{lo}$  is the researcher's generated single phase inside-pipe condenser heat transfer coefficient.

### 3.3 Void Fraction

The void fraction is defined as the time-averaged volumetric fraction of vapour in the two-phase mixture. The volume of each phase is equal to the cross-sectional area of the phase flow multiplied by a differential length element. The general equation for the void fraction is given as [7]:

$$\alpha = \frac{1}{1 + \left( S \frac{1-x}{x} \frac{\rho_g}{\rho_l} \right)} \quad (19)$$

Saha [10] recommends the commonly used Modified Smith model:

$$S = K + (1 + K) \left\{ \frac{\frac{\rho_l}{\rho_v} + K \left( \frac{1}{x} - 1 \right)}{1 + K \left( \frac{1}{x} - 1 \right)} \right\}^{0.5} \quad (20)$$

Where:

$$K = 0.95 \tanh(5x) + 0.05 \quad (21)$$

### 3.4 Two Phase Multiplier

Saha [11] recommends the Martinelli-Nelson correlation for water:

$$\phi_{Lo}^2 = (1 - x)^{1.75} \phi_L^2 \quad (22)$$

In equation 22,  $\phi_L^2$  refers to the Lockhart-Martinelli correlation for the two-phase multiplier for liquid phase friction [11]:

$$\phi_L^2 = \left(1 + \frac{20}{x} + \frac{1}{x^2}\right)^{0.5} \quad (23)$$

X in the above equation is the Martinelli parameter given by the following correlation, assuming both phases are turbulent [11]:

$$X_{tt} = \left(\frac{1-x}{x}\right)^{0.9} \left(\frac{\rho_v}{\rho_l}\right)^{0.5} \left(\frac{\mu_l}{\mu_v}\right)^{0.1} \quad (24)$$

## 4. RESULTS

A computer program was written using PowerBasic Compiler 9.0 (copyright 2008). Results from the computer program were imported into Microsoft Excel which was used to generate graphs.

Figure 5 shows a comparison between the theoretically and experimentally determined mass flow rates of the working fluid for single to two-phase operating mode. The experimentally determined mass flow rate, depicted in grey, increases steadily in the single phase region and stabilises at 17.98 mg/s for 30% power, 39.5 mg/s for 50% power and 61.2 mg/s for 70% power. Each increase of power input results in a relatively small peak in mass flow rate. The heat transferred to the working fluid is directly proportional to the difference in fin and bulk fluid temperature, as well as the flow rate. The instant the power is increased, the temperature difference is unchanged, resulting in an increased mass flow rate. At the onset of subcooled nucleate boiling, the mass flow rate drops sharply. During subcooled boiling, the wall temperature

exceeds the bulk fluid temperature. Bubbles form at nucleation sites on the tube wall but, due to the cooler core bulk temperature, remain affixed to the wall [5]. Once the bubbles break free, the cooler fluid temperature forces the vapour to condense, collapsing the bubble. While these bubbles line the tube wall they act as flow restrictions, increasing the wall friction and thus decreasing the working fluid flow rate. Once the nucleate boiling becomes saturated, the mass flow rate starts oscillating with a relatively large amplitude. The oscillations can be attributed to the varying driving force as a result of pressure differences between the heated and cooled section.

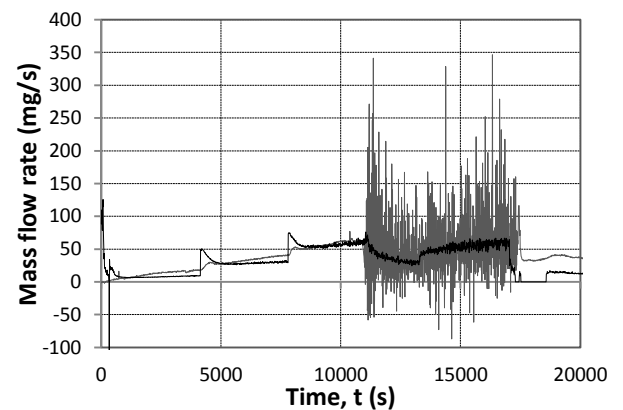


Figure 5: Comparison of theoretically and experimentally determined mass flow rate

The theoretically determined mass flow rate, depicted in black in figure 5, very closely predicts the experimental profile. In the two-phase region, the experimental profile follows a similar trend with almost identical average values without capturing the oscillations.

## 5. DISCUSSIONS AND CONCLUSIONS

The most widely used two-phase flow models in the nuclear industry are the 3-equation models. The homogenous equilibrium model, which assumes that the two fluid phases behave as a flowing mixture, was selected for the numerical simulation model.

A one-third-height-scale model of the RCCS was designed and manufactured which was used to perform twelve experiments, lasting at least 5 hours each, with data logging occurring every ten seconds.

The RCCS was modelled as a one-dimensional system, making several assumptions: the thermodynamic process is quasi-static; compressibility effects due to heating or cooling of the liquid and vapour phases are negligible; and the flow is one-dimensional. Correlations for the friction factor, heat transfer coefficient, void fraction and two-phase frictional multiplier were identified. Due to the lack of relevant natural flow correlations, most of the correlations used are for forced flow. This introduces room for over- or under- prediction of the model as the working fluid flow might not be fully developed at all times.

The resulting numerical model was used to simulate the RCCS and predict the working fluid mass flow rate during single and two-phase operation.

Shortcomings identified in the theoretical model are:

- Using the electrical power input in  $Re_q$  in the generated evaporator heat transfer coefficient correlations yields an inaccurate trend in the results.
- General frictional loss coefficient correlations were used rather than correlations specific to the various flow patterns.
- The large number of variables and temperature dependant functions used, limited the choice of programming language for a computer model. QuickBasic allowed for acceptable processing speed without simplifying these functions.
- One-dimensional analysis was used. Though analysis in more dimensions could offer more accurate results, the trade off is more complicated

correlations, more assumptions, more restrictions and constitutive laws required. Not only would this exponentially increase the processing time, it also increases the room for error. The vast amount of literature available and thorough understanding of one-dimensional analysis allows the researcher to focus on heat transfer coefficient correlations in the theoretical modelling.

In conclusion, the comparison between experimental and theoretical results shows that the numerical model closely predicts experimental data and hence can be used in confidence for design purposes.

## NOMENCLATURE

$A$	area, $m^2$
$c$	specific heat, $J/kg\ K$
$D$	pipe diameter, $m$
$f$	Darcy friction factor
$g$	gravitational constant, $m/s^2$
$Gr$	Grashof number
$h$	heat transfer coefficient, $W/m^2\ K$
$k$	thermal conductivity, $W/m\ K$
$K$	minor loss coefficient
$L$	length, $m$
$\dot{m}$	mass flux, $kg/s$
$Nu$	Nusselt number
$P$	Pressure, $Pa$
$Pr$	Prandtl number
$q$	thermal energy, $J$
$Re$	Reynolds number
$S$	slip
$T$	temperature, $K$ or $^{\circ}C$
$t$	time, $s$
$v$	phase velocity, $m/s$
$V$	velocity, $m/s$
$X$	Martinelli parameter
$x$	thermodynamic quality

## Greek letters

$\alpha$	vapour void fraction
$\beta$	thermal expansion coefficient, $K^{-1}$
$\theta$	angle, $rad$
$\lambda$	thermal conductivity
$\mu$	dynamic viscosity, $kg/m\ s$

$\rho$	density, kg/m <sup>3</sup>
$\sigma$	surface tension, N/m
$\tau$	shear stress, N/m <sup>2</sup>
$\varphi$	fluid phase parameter
$\Phi^2$	two phase multiplier
$\nu$	kinematic viscosity, kg/ms

Superscript  
 $\circ$  stagnation

Subscript	
$a$	air
$b$	bulk
$C$	cold
$c$	convection
$cw$	cooling water
$D$	diameter
$e$	evaporator
$et$	expansion tank
$f$	saturated liquid
$FC$	forced convection
$fg$	latent
$g$	generated, gas
$H$	hot
$i$	inside
$k$	denotes phase
$k$	conduction
$l$	liquid phase
$l$	laminar
$lo$	liquid only
$m$	mixture
$o$	outside
$p$	constant pressure
$r$	reduced
$s$	surface
$sat$	saturated
$t$	turbulent
$tt$	turbulent-turbulent
$v$	constant volume
$v$	gaseous phase
$w$	water, wall
$x$	cross-sectional

## References

1. van Staden, M. (2001). *Analysis of effectiveness of the PBMR cavity cooling system*. South Africa: PBMR Ltd (Pty).
2. Dobson, R., and Ruppensburg, J. (2006). Experimental evaluation of the flow and heat transfer in a closed loop thermosyphon. *JESA*.
3. Reyes, J. (2007). *Governing Equations in Two-Phase Fluid Natural Circulation*. Vienna: International Atomic Energy Agency.
4. Çengel, Y. (2003). *Heat Transfer A Practical Approach Second Edition*. New York: McGraw-Hill Companies, Inc.
5. Whalley, P. (1987). *Boiling, condensation and gas-liquid flow*. Oxford: Clarendon Press.
6. Crowe, C., Elger, D., & Roberson, J. (2001). *Engineering Fluid Mechanics 7th Edition*. New York: John Wiley & Sons. Inc.
7. Mills, A. (1999). *Heat Transfer, 2nd ed.* Upper Saddle River: Prentice Hall.
8. Collier, J., and Thome, J. (1994). *Convective boiling and condensation, 3rd ed.* Oxford: Clarendon press.
9. Shah, M. (1989). A general correlation for heat transfer during film condensation inside pipes. *International Journal of Heat and Mass Transfer, Vol. 22*, 547-556.
10. Saha, D. (June 2009). Local Phenomena Associated With Natural Circulation. *IAEA-UNIP Training Course on Natural Circulation Phenomena and Modelling in Water Cooled Nuclear Power Plants*, (p. Lecture Notes T4 and T5 ). Pisa.
11. Carey, V. (1992). *Liquid-Vapour Phase Change Phenomena: An Introduction to the Thermodynamics of Vaporization and Condensation Processes in Heat Transfer Equipment*. Washington: Hemisphere Publishing Corporation.